

AD-A078 750

OHIO STATE UNIV COLUMBUS ELECTROSCIENCE LAB  
POINTING ACCURACY AND DYNAMIC RANGE IN A STEERED BEAM ADAPTIVE --ETC(U)  
NOV 79 R T COMPTON N00019-79-C-0291  
ESL-711847-4 NL

UNCLASSIFIED

1 OF 1  
AD  
80 78750

END  
DATE  
FILMED  
1-80  
DRC

OSU

The Ohio State University

POINTING ACCURACY AND DYNAMIC RANGE  
IN A STEERED BEAM ADAPTIVE ARRAY

R. T. Compton, Jr.

**LEVEL**

12  
APPROVED FOR PUBLIC RELEASE;  
DISTRIBUTION UNLIMITED

The Ohio State University

**ElectroScience Laboratory**

Department of Electrical Engineering  
Columbus, Ohio 43212

DDC  
REFILIT  
JAN 15 1980  
E

ADA 078750

Technical Report 711847-4

November 1979

This document has been approved  
for public release and sale; its  
distribution is unlimited.

DDC FILE COPY

Naval Air Systems Command  
Washington, D.C. 20361

80 1 - 9 001

## NOTICES

When Government drawings, specifications, or other data are used for any purpose other than in connection with a definitely related Government procurement operation, the United States Government thereby incurs no responsibility nor any obligation whatsoever, and the fact that the Government may have formulated, furnished, or in any way supplied the said drawings, specifications, or other data, is not to be regarded by implication or otherwise as in any manner licensing the holder or any other person or corporation, or conveying any rights or permission to manufacture, use, or sell any patented invention that may in any way be related thereto.

REPORT DOCUMENTATION PAGE		READ INSTRUCTIONS BEFORE COMPLETING FORM
1. REPORT NUMBER	2. GOVT ACCESSION NO.	3. RECIPIENT'S CATALOG NUMBER
4. TITLE (and Subtitle) (6) <u>POINTING ACCURACY AND DYNAMIC RANGE</u> <u>IN A STEERED BEAM ADAPTIVE ARRAY</u>		5. TYPE OF REPORT & PERIOD COVERED (9) Technical Report
7. AUTHOR(s) (10) R. T. Compton, Jr.		6. PERFORMING ORG. REPORT NUMBER (14) ESL-711847-4
9. PERFORMING ORGANIZATION NAME AND ADDRESS The Ohio State University ElectroScience Laboratory, Department of Electrical Engineering Columbus, Ohio 43212		8. CONTRACT OR GRANT NUMBER(s) (15) Contract N00019-79-C-0201
11. CONTROLLING OFFICE NAME AND ADDRESS Naval Air Systems Command Washington, D.C. 20361		10. PROGRAM ELEMENT, PROJECT, TASK AREA & WORK UNIT NUMBERS (12) 34
14. MONITORING AGENCY NAME & ADDRESS (if different from Controlling Office)		12. REPORT DATE (11) Nov 1979
		13. NUMBER OF PAGES 30
		15. SECURITY CLASS. (of this report) Unclassified
		15a. DECLASSIFICATION/DOWNGRADING SCHEDULE
16. DISTRIBUTION STATEMENT (of this Report)  <b>APPROVED FOR PUBLIC RELEASE; DISTRIBUTION UNLIMITED</b>		
17. DISTRIBUTION STATEMENT (of the abstract entered in Block 20, if different from Report)  JAN 16 1980		
18. SUPPLEMENTARY NOTES		
19. KEY WORDS (Continue on reverse side if necessary and identify by block number) Adaptive arrays Communications Interference rejection		
20. ABSTRACT (Continue on reverse side if necessary and identify by block number) This report examines the performance of a steered beam adaptive array as a function of the beam pointing error. The purpose is to determine how close the steered beam has to be to the actual desired signal arrival angle for good performance. It is shown that the beam pointing error that can be tolerated is essentially a question of dynamic range. The greater the desired signal dynamic range that must be accommodated by the array, the more accurate the beam pointing angle must be.		

# CONTENTS

	Page
I. INTRODUCTION	1
II. FORMULATION OF THE PROBLEM	4
III. RESULTS	11
IV. CONCLUSIONS	24
REFERENCES	30

Accession For	
NTIS GAA&I	<input checked="checked" type="checkbox"/>
DDC TAB	<input type="checkbox"/>
Unannounced	<input type="checkbox"/>
Justification	
By _____	
Distribution/	
Availability/	
Dist	Availability/
A	special

## I. INTRODUCTION

Desired signal tracking with an adaptive array can be accomplished two ways. One can either supply a reference signal in the array feedback loop, and use the LMS algorithm of Widrow, et al [1], or one can inject steering weights into the feedback loops, as originally suggested by Applebaum [2].

In the LMS array[1], the mean-square difference between the array output signal and a reference signal [3,4,5] (or "desired response"[1]) is minimized by the array feedback. When the reference signal is correlated with the desired signal (and uncorrelated with the interference), the array automatically maintains a strong pattern response in the desired signal direction. Usually the result is a beam that tracks the desired signal.

However, generating a reference signal for the LMS array can be a difficult task. Several problems confront the designer. First, there must be some way to process the array output signal so the desired signal is preserved and the interference is decorrelated. Second, there is usually an acquisition problem. The frequency of the incoming desired signal, and often the timing of a pseudonoise code or other tagging modulation, are unknown and must be determined before reference signal generation can begin. Third, it must be possible to start reference signal generation in the presence of interference and before the array nulls the desired signal. Finally, generating the reference signal usually requires a great deal of electronic circuitry behind the array. Although suitable reference signal generation techniques have been found for a few types of communication systems [4,5], for many other types of systems, there simply does not appear to be any way to generate a reference signal.

The second way to steer the beam in an adaptive array is to insert steering weights into the array feedback loops, as described by Applebaum[2]. This approach is vastly simpler, since no reference signal is required at all. The only difficulty with this approach is that the designer must know where to point the beam. He must know the desired signal arrival angle.

When the desired signal arrival angle is unknown, one can still use the Applebaum array, in the form of a power inversion array[6], to obtain some interference protection. A power inversion array is just an Applebaum array with a steering vector that turns one element on and the rest off. The element turned on is chosen so its element pattern covers some large sector of space from which desired signals may arrive. There is no attempt to steer a beam toward the desired signal.

However, the performance of a power inversion array is much poorer than that of the Applebaum array with a properly steered beam. For example, a power inversion array can accommodate only a limited dynamic range for the desired signal [6]. If the desired signal is too strong, the array will null it.

Because of the simplicity of the steered beam array, compared to the LMS array with a reference signal, it is certainly the most desirable approach if the desired signal arrival angle is known. In many design situations, the signal angle may be known approximately, but not exactly. Or, it may be possible to estimate the signal angle[7]. For this reason, it is of interest to determine how well a steered beam array will perform when the beam pointing angle is in error. That is the subject we address here.

In this report, we examine the performance of a two-element steered beam adaptive array as a function of the beam pointing error. We include in our model the effects of desired signal-to-noise ratio, interference-to-noise ratio, feedback loop gain, signal arrival angles, and signal bandwidths. We will show several things. First, we will note that to obtain full gain from the array when the signal power is high, the beam angle must be extremely close to the correct direction. (This fact has been pointed out previously by Zahm[8].) Second, we will find that the pointing error that can be tolerated is essentially a question of dynamic range; the greater the desired signal dynamic range that must be accommodated by the array, the smaller the pointing error must be. Third, we will compare the steered beam array performance with that of a power inversion array and an LMS array. We will find that the steered beam array performs better than the power inversion array even with quite large steering errors, but poorer than the LMS array for any nonzero pointing error. Finally, we will show that with interference present, the performance of the two-element array is less sensitive to pointing errors than without the interference.

In Section II of the report, we define the model for the problem and formulate the necessary equations. In Section III, we present calculated results. Section IV contains the conclusions.



## II. FORMULATION OF THE PROBLEM

Consider the 2-element adaptive array shown in Figure 1. The elements are assumed isotropic and a half wavelength apart. The complex (analytic) signal  $\tilde{x}_i(t)$  from each element is multiplied by a complex weight  $w_i$  and summed to produce the array output  $\tilde{s}(t)$ . The array weights are assumed controlled by feedback loops as described by Applebaum [2], which are also known as power inversion loops [6]. In such an array, the steady-state weight vector  $w = (w_1 \ w_2)^T$  is given by [2,6]

$$w = [I + k\Phi]^{-1} w_0, \quad (1)$$

where  $\Phi$  is the covariance matrix,

$$\Phi = E(X^*X^T), \quad (2)$$

and  $w_0$  is the steering vector

$$w_0 = (w_{10}, w_{20})^T. \quad (3)$$

In these equations,  $I$  is the identity matrix,  $k$  is the feedback loop gain [6],  $T$  denotes the transpose, and "\*" is complex conjugate.  $X$  is the signal vector

$$X = (\tilde{x}_1(t), \tilde{x}_2(t))^T, \quad (4)$$

and  $E(.)$  denotes the expectation.

Suppose two signals are incident on the array, one desired and one interference. Also, suppose thermal noise is present on each element signal. Then the element signals are

$$\tilde{x}_j(t) = \tilde{d}_j(t) + \tilde{i}_j(t) + \tilde{n}_j(t), \quad j = 1, 2 \quad (5)$$

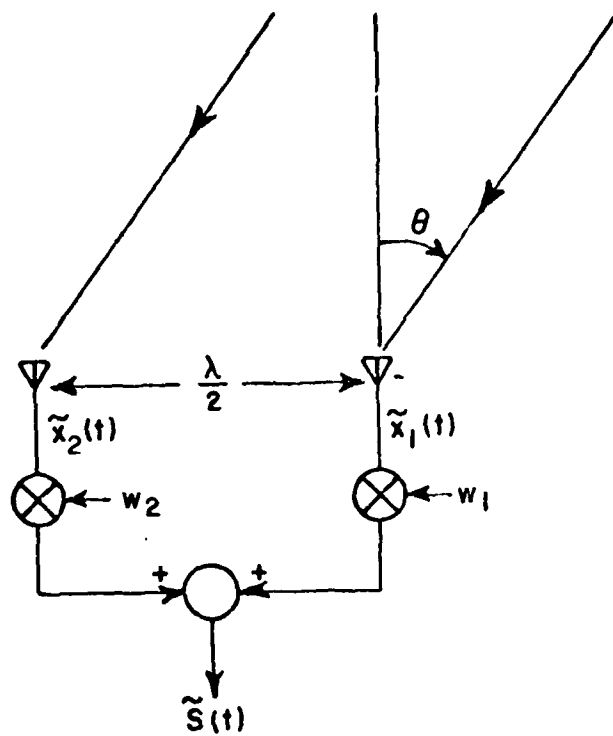


Figure 1. Two-element adaptive array.

where  $\tilde{d}_j(t)$  is the desired signal,  $\tilde{i}_j(t)$  is the interference, and  $\tilde{n}_j(t)$  is the noise. The  $\tilde{n}_j(t)$  are assumed zero-mean, bandlimited gaussian noise signals with

$$E[\tilde{n}_i(t) \tilde{n}_j^*(t)] = \sigma^2 \delta_{ij} , \quad (6)$$

where  $\delta_{ij}$  is the Kronecker delta.

We assume the desired signals  $\tilde{d}_1(t)$  and  $\tilde{d}_2(t)$  differ only by an interelement propagation time delay  $T_d$ , i.e.,

$$\tilde{d}_1(t) = \tilde{d}(t), \quad (7a)$$

$$\tilde{d}_2(t) = \tilde{d}(t - T_d), \quad (7b)$$

where  $\tilde{d}(t)$  is the desired signal waveform and  $T_d$  is

$$T_d = \frac{\ell}{c} \sin \theta_d , \quad (8)$$

with  $\ell$  the element separation,  $c$  the velocity of propagation, and  $\theta_d$  the arrival angle, relative to broadside. Similarly, we assume

$$\tilde{i}_1(t) = \tilde{i}(t) , \quad (9a)$$

$$\tilde{i}_2(t) = \tilde{i}(t - T_i) , \quad (9b)$$

where  $\tilde{i}(t)$  is the interference waveform and

$$T_i = \frac{\ell}{c} \sin \theta_i , \quad (10)$$

with  $\theta_i$  the interference arrival angle. Also, we assume the desired and interference signals are zero-mean, stationary, and statistically independent of each other and the thermal noise.

With these assumptions, the covariance matrix in Equation (2) is

$$\Phi = \sigma^2 I + \begin{pmatrix} R_d(0) + R_i(0) & R_d^*(T_d) + R_i^*(T_i) \\ R_d(T_d) + R_i(T_i) & R_d(0) + R_i(0) \end{pmatrix}, \quad (11)$$

where  $R_d(\tau)$  and  $R_i(\tau)$  are the autocorrelation functions of  $\tilde{d}(t)$  and  $\tilde{i}(t)$ :

$$R_d(\tau) = E[\tilde{d}(t+\tau)\tilde{d}^*(t)], \quad (12a)$$

$$R_i(\tau) = E[\tilde{i}(t+\tau)\tilde{i}^*(t)]. \quad (12b)$$

It is convenient to define

$$S_d = R_d(0) = \text{desired signal power per element}, \quad (13a)$$

$$S_i = R_i(0) = \text{interference signal power per element}, \quad (13b)$$

and also the normalized autocorrelations

$$\rho_d = \frac{R_d(T_d)}{S_d}, \quad (14a)$$

$$\rho_i = \frac{R_i(T_i)}{S_i}. \quad (14b)$$

In addition, we define the normalized parameters

$$K = k\sigma^2 = \text{normalized loop gain}, \quad (15a)$$

$$\xi_d = \frac{S_d}{\sigma^2} = \text{desired signal-to-noise ratio (SNR) per element}, \quad (15b)$$

$$\xi_i = \frac{S_i}{\sigma^2} = \text{interference-to-noise ratio (INR) per element}. \quad (15c)$$

The matrix  $I+k\Phi$  may then be written

$$I+k\Phi = \begin{pmatrix} 1+K+K\xi_d+K\xi_i & K\xi_d\rho_d^*+K\xi_i\rho_i^* \\ K\xi_d\rho_d+K\xi_i\rho_i & 1+K+K\xi_d+K\xi_i \end{pmatrix}. \quad (16)$$

The inverse of this is

$$[I+k\Phi]^{-1} = \frac{1}{D} \begin{pmatrix} 1+K+K\xi_d+K\xi_i & -K\xi_d\rho_d^*-K\xi_i\rho_i^* \\ -K\xi_d\rho_d-K\xi_i\rho_i & 1+K+K\xi_d+K\xi_i \end{pmatrix}, \quad (17)$$

where  $D$  is the determinant of  $I+k\Phi$ :

$$D = (1+K+K\xi_d+K\xi_i)^2 - |K\xi_d\rho_d+K\xi_i\rho_i|^2. \quad (18)$$

The steady-state weights in the array may now be determined from Equation (1) for any given steering vector  $w_0$ .

In this report we assume the steering vector  $w_0$  is chosen to provide a beam maximum of the quiescent pattern in a given direction  $\theta_{\max}$ . To determine  $w_0$ , we note that a CW signal from an angle  $\theta_{\max}$  will produce a signal vector

$$x = \begin{pmatrix} 1 & e^{-j\pi \sin \theta_{\max}} \end{pmatrix}^T e^{j\omega_0 t}. \quad (19)$$

The array output from such a signal would be

$$\tilde{s}(t) = x^T w = \begin{pmatrix} w_1 + w_2 e^{-j\pi \sin \theta_{\max}} \end{pmatrix} e^{j\omega_0 t}. \quad (20)$$

The array will have a pattern maximum on this signal if

$$w_1 = w_2 e^{-j\pi \sin \theta_{\max}}. \quad (21)$$

Hence, for a given  $\theta_{\max}$ , we choose\*

$$w_0 = \begin{pmatrix} e^{-j\pi \sin \theta_{\max}} & 1 \end{pmatrix}^T. \quad (22)$$

From this  $w_0$ , the steady-state weight vector  $w$  may then be calculated from Equation (1) using  $[I+k\Phi]^{-1}$  from Equation (17).

To proceed, we must first define the signals  $\tilde{d}(t)$  and  $\tilde{i}(t)$  so  $\rho_d$  and  $\rho_i$  may be found. We will assume the desired signal and the interference are each stochastic processes with a flat bandlimited power spectral density centered at  $\omega_0$ . The desired signal will have bandwidth  $\Delta\omega_d$ , so its autocorrelation function is

$$R_d(\tau) = S_d \frac{\sin(\frac{\Delta\omega_d \tau}{2})}{(\frac{\Delta\omega_d \tau}{2})} e^{j\omega_0 \tau}. \quad (23)$$

Substituting  $\tau=T_d$  and noting that

$$\frac{\Delta\omega_d T_d}{2} = \frac{1}{2} \left( \frac{\Delta\omega_d}{\omega_0} \right) (\omega_0 T_d) = \frac{1}{2} B_d \phi_d, \quad (24)$$

where  $B_d$  is the fractional bandwidth,

$$B_d = \frac{\Delta\omega_d}{\omega_0}, \quad (25)$$

and  $\phi_d$  is the interelement phase shift for the desired signal,

$$\phi_d = \omega_0 T_d, \quad (26)$$

we have

$$\rho_d = \frac{\sin \frac{1}{2}(B_d \phi_d)}{\frac{1}{2}(B_d \phi_d)} e^{j\phi_d}. \quad (27)$$

\*In a power inversion array [2], where we have no information about desired signal arrival angle, we instead choose  $w_0 = (1, 0)^T$ . This choice makes the quiescent pattern omnidirectional.

Similarly, if the interference has bandwidth  $\Delta\omega_i$ , we define the fractional bandwidth

$$B_i = \frac{\Delta\omega_i}{\omega_0} , \quad (28)$$

and phase shift

$$\phi_i = \omega_0 T_i . \quad (29)$$

Then

$$\rho_i = \frac{\sin \frac{1}{2}(B_i \phi_i)}{\frac{1}{2}(B_i \phi_i)} e^{j\phi_i} . \quad (30)$$

From  $w$  in Equation (1), the array output desired signal power, interference power and thermal noise power may now be calculated. The desired signal at the array output is

$$\tilde{s}_d(t) = [\tilde{d}(t), \tilde{d}(t-T_d)] w . \quad (31)$$

The output desired signal power is then

$$\begin{aligned} P_d &= \frac{1}{2} E [\tilde{s}_d^*(t) \tilde{s}_d(t)] \\ &= \frac{1}{2} S_d [|w_1|^2 + |w_2|^2 + 2\text{Re}\{w_1 w_2^* \rho_d\}] . \end{aligned} \quad (32)$$

The output interference signal is

$$\tilde{s}_i(t) = [\tilde{i}(t), \tilde{i}(t-T_i)] w , \quad (33)$$

and the output interference power is

$$P_i = \frac{1}{2} S_i [|w_1|^2 + |w_2|^2 + 2\text{Re}\{w_1 w_2^* \rho_i\}] . \quad (34)$$

The output thermal noise signal is

$$\tilde{s}_n(t) = [\tilde{n}_1(t), \tilde{n}_2(t)] w . \quad (35)$$

The output thermal noise power is simply (in view of Equation (6)):

$$P_n = \frac{\sigma^2}{2} [|w_1|^2 + |w_2|^2] \quad (36)$$

From  $P_d$ ,  $P_i$  and  $P_n$  we may compute the output desired signal-to-interference-plus-noise ratio (SINR):

$$\text{SINR} = \frac{P_d}{P_i + P_n} \quad (37)$$

which we use as a measure of array performance in the sequel.

We now have all the equations needed to compute the output SINR as a function of  $\theta_d$ ,  $B_d$ ,  $\xi_d$ ,  $\theta_i$ ,  $B_i$ ,  $\xi_i$  and  $\theta_{\max}$ . In the next section we give the results of such calculations and show what happens to array performance when  $\theta_{\max} \neq \theta_d$ .

### III. RESULTS

Our purpose is to learn how well the array performs when  $\theta_{\max}$ , the beam pointing angle, is not equal to  $\theta_d$ , the desired signal arrival angle. Consider first the case where there is no interference ( $\rho_i=0$ ). Figure 2 shows the output SINR from the array as a function of  $\theta_{\max}$  when  $\theta_d=0^\circ$ . Several curves are shown for different SNRs (input desired signal-to-noise ratios). The curves are computed for  $K=0.1$  and  $B_d=0$ . ( $B_d$  is found to have no effect on the results. The choice of  $K$  will be discussed below.)

From these curves, we see that the higher the SNR, the closer  $\theta_{\max}$  must be to  $\theta_d$  to achieve maximum gain from the array. For example, if  $\text{SNR}=0$  dB, the array provides better than 0 dB gain (i.e.,  $\text{SINR} > 0$  dB) as long as  $-27^\circ < \theta_{\max} < 27^\circ$ , but for  $\text{SNR}=20$  dB, the array gain exceeds



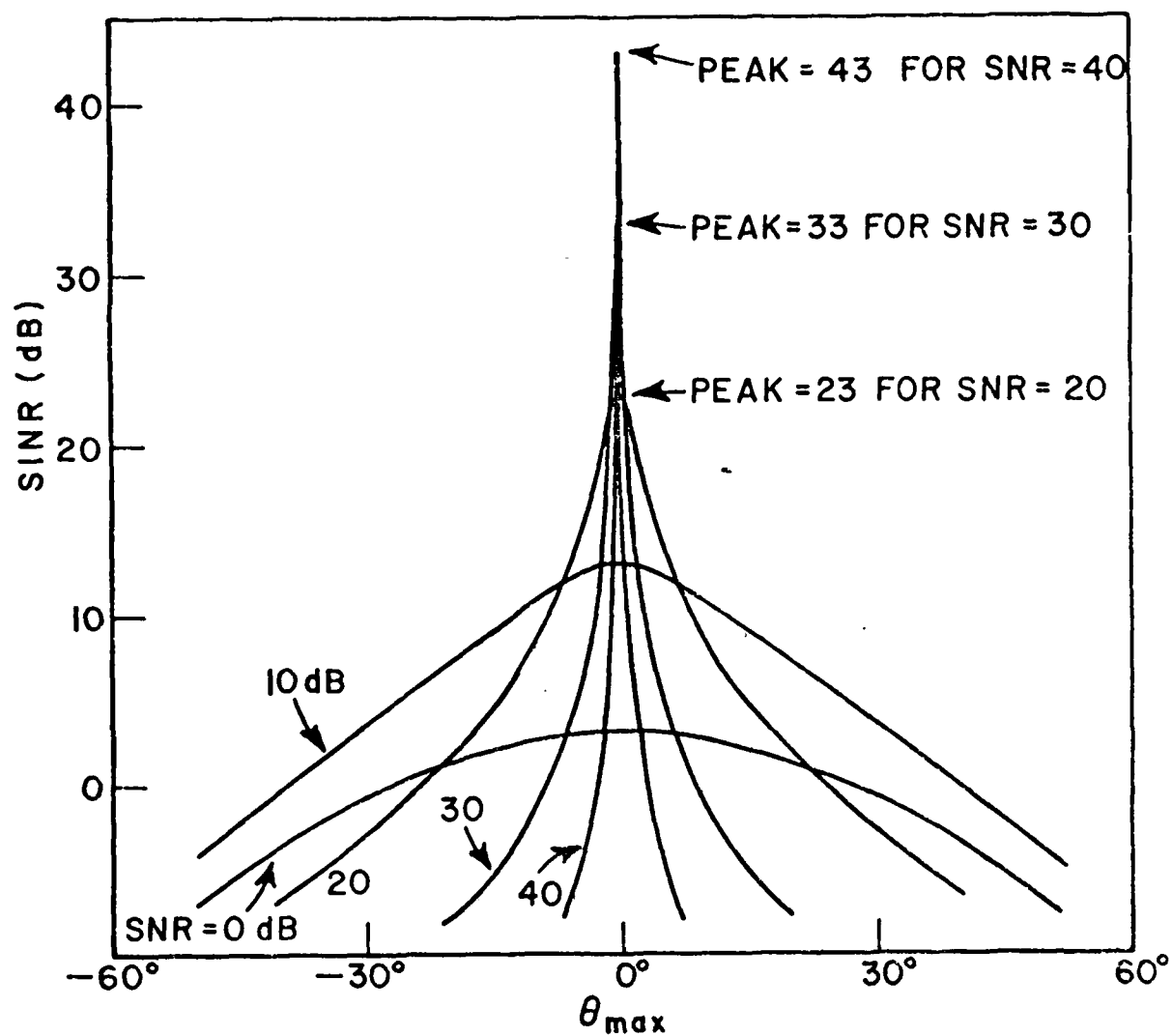


Figure 2. SINR vs.  $\theta_{max}$ .  
 $\theta_d = 0^\circ$ ,  $K = .1$ ,  $B_d = 0$ .  
 No interference.

0 dB ( $\text{SINR} > 20$  dB) only if  $-2^\circ < \theta_{\max} < 2^\circ$ .\* Of course, for most system designs, achieving maximum gain is not the most important question. What matters is achieving a given minimum SINR at the array output. However, the trend is the same. For example, if  $\text{SNR} = 10$  dB, we require  $-39^\circ < \theta_{\max} < 39^\circ$  to achieve  $\text{SINR} > 0$  dB. But for  $\text{SNR} = 30$  dB,  $-8.8^\circ < \theta_{\max} < 8.8^\circ$  is necessary for  $\text{SINR} > 0$  dB.

The behavior of the curves in Figure 2 may be understood by examining the array patterns. Figures 3 and 4 show some typical patterns under the same conditions as in Figure 2. In Figure 3,  $\theta_{\max}$  is  $0^\circ$  and in Figure 4,  $\theta_{\max}$  is  $10^\circ$ . For  $\theta_{\max} = 0^\circ$ , we find that as the SNR increases, the overall pattern magnitude is reduced. The array does not try to null the desired signal. As the pattern amplitude drops, both the desired signal power and the thermal noise power drop in proportion. Hence the output SINR remains unaffected by this change in pattern amplitude.

For  $\theta_{\max} = 10^\circ$ , however, the pattern behavior is quite different. Now as the SNR increases, the array increasingly nulls the desired signal. Since it can do this without lowering the overall pattern amplitude, the result is to reduce the desired signal power without reducing the thermal noise power. Hence, the SINR drops as the SNR increases. This accounts for the behavior seen in Figure 2.

In general, we find that the closer  $\theta_{\max}$  is to the desired signal direction  $\theta_d$ , the stronger the desired signal power must be to move the null on to the desired signal.

---

\*This sharp dependence of SINR on pointing error has been noted previously by Zahm [8], who showed similar results for a four-element linear array.

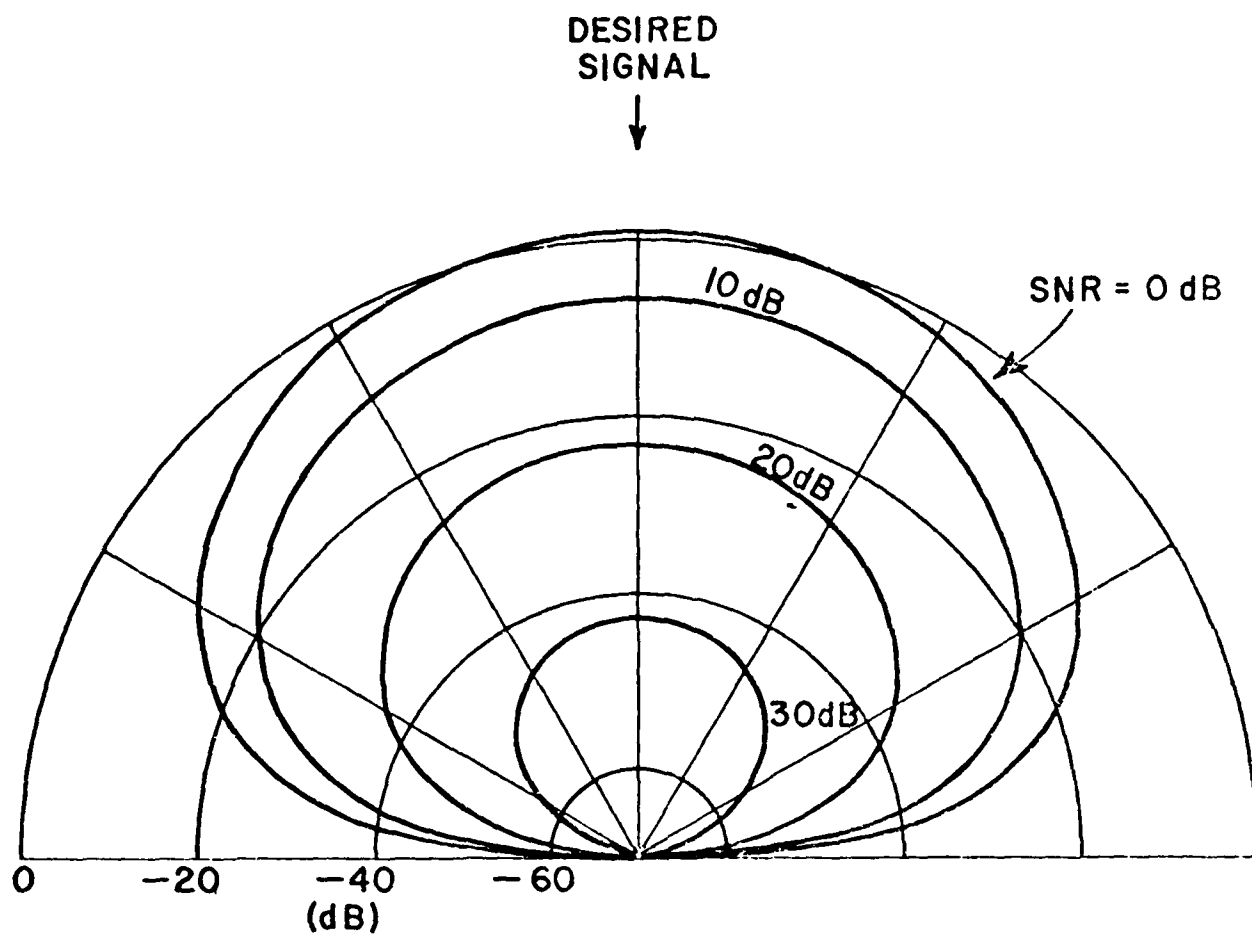


Figure 3. Array pattern.

$K=0.1$ ,  $\theta_d=0$ ,  $B_{\max}=0$ .

No interference.

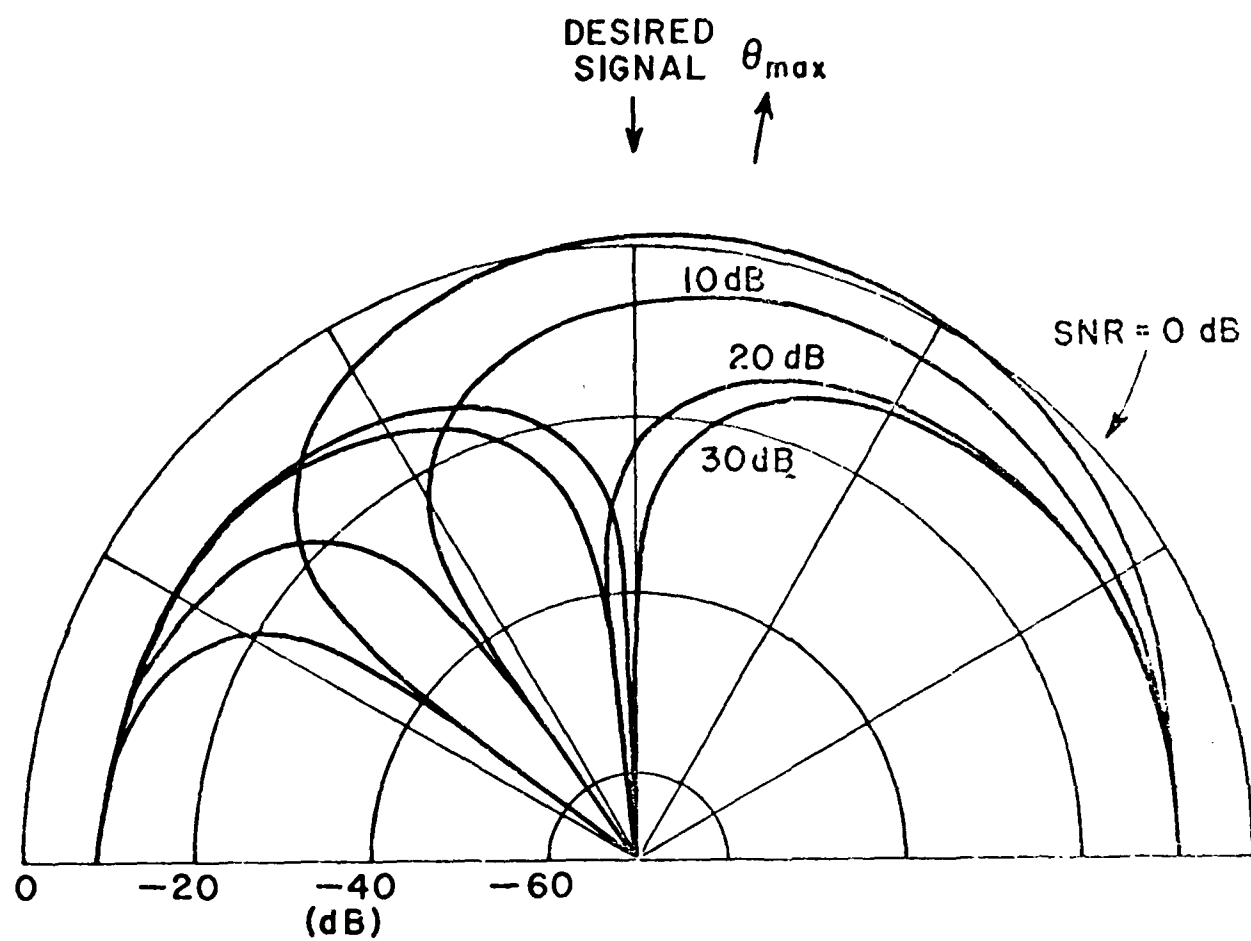


Figure 4. Array pattern.  
 $K=0.1$ ,  $B_d=0$ ,  $\theta_{\max}=10^\circ$ .  
 No interference.

A different perspective on these results may be gained by plotting the SINR versus the SNR. This is done for several values of  $\theta_{\max}$  in Figure 5. This figure is interesting because it immediately shows that the beam pointing that can be tolerated is essentially a matter of dynamic range. For example, if  $\theta_{\max} = 10^\circ$ , we have  $\text{SINR} > 0$  dB only for  $-3 \text{ dB} < \text{SNR} < 29 \text{ dB}$ , whereas if  $\theta_{\max} = 1^\circ$ ,  $\text{SINR} > 0$  dB for  $-3 \text{ dB} < \text{SNR} < 49 \text{ dB}$ . The greater the desired signal dynamic range we wish to accommodate, the closer  $\theta_{\max}$  must be to the desired signal angle.

Also shown in Figure 5 is the performance achieved by a power inversion array, with  $w_0 = (1, 0)^T$ , under the same conditions\*. It turns out that the power inversion array has the same performance as the steered beam array with  $\theta_{\max} = 30^\circ$ . The performance of the steered beam array is thus seen to exceed that of the power inversion array as long as  $-30^\circ < \theta_{\max} < 30^\circ$ .

We note also that an LMS array, using a replica of the desired signal as the reference signal, has essentially the same performance as the curve shown for  $\theta_{\max} = 0^\circ$  in Figure 5.\*\* Thus, the performance

---

\*The calculation of SINR for the power inversion array, is carried out in Reference 6.

\*\*For the LMS array, the steady-state weights are  $w = \Phi^{-1}s$ , where  $S = E\{XR(t)\}$ , with  $R(t)$  the reference signal, and  $\Phi$  is the covariance matrix in Equation (2) [1]. When  $R(t)$  is correlated with the desired signal,  $S$  is a vector parallel to  $w_0 = (1, 1)$ , i.e., the same as the steering vector with  $\theta_{\max} = 0^\circ$ . Hence the only difference between the LMS weights and those used here is due to the  $I$  term in Equation (1). This term makes a negligible difference on the output SINR computed in Figure 5.

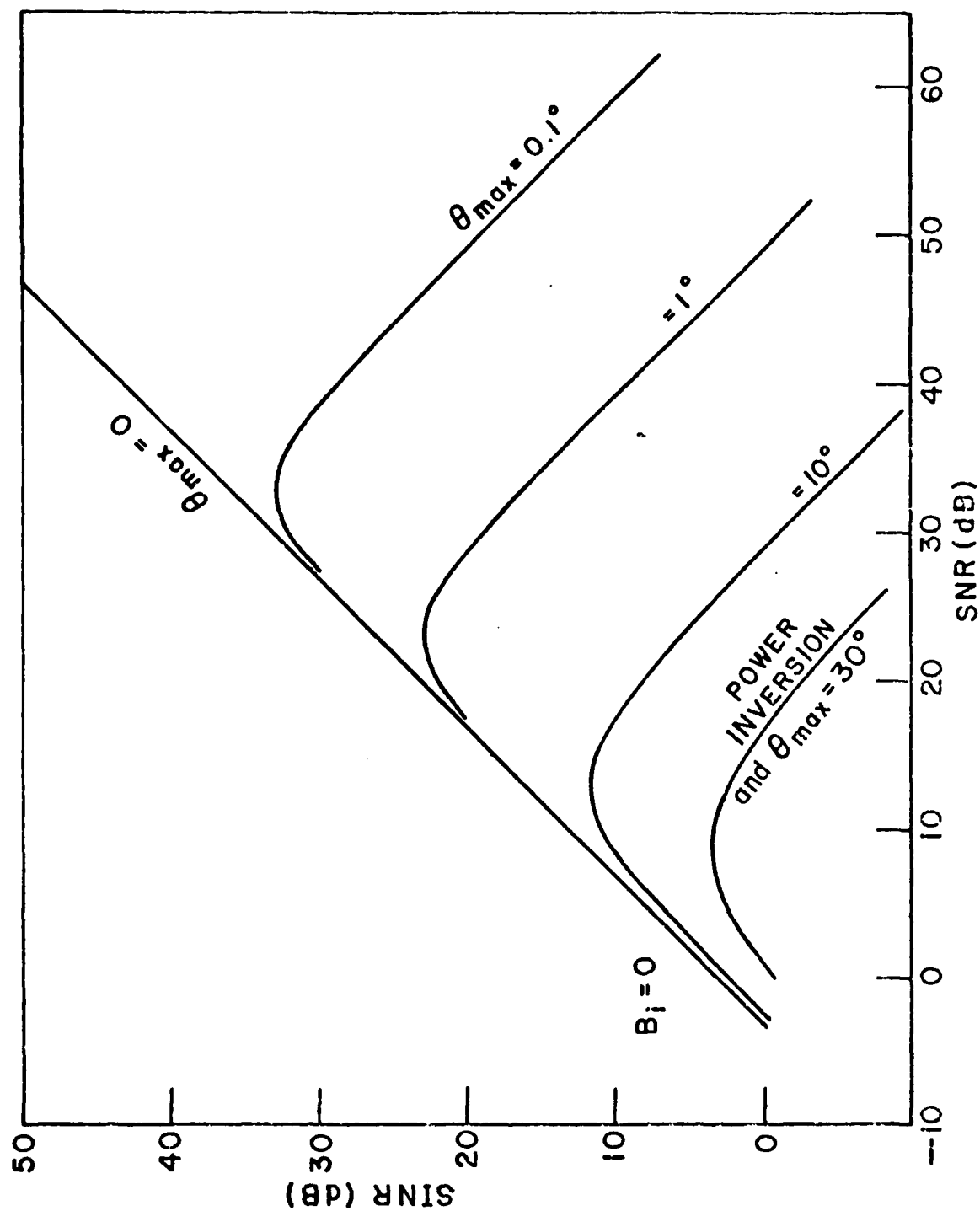


Figure 5. Steered beam array performance  
 $\theta_d = 0^\circ$ ,  $\theta_i = 50^\circ$ ,  $K = 1$ ,  $B_d = 0$ , No interference.

of the steered beam array approaches that of the LMS array as the pointing error goes to zero.

The previous curves were all for a loop gain of  $K=0.1$ . The effect of loop gain on these results is illustrated in Figure 6, which shows typical curves of SINR versus  $K$ , for  $\text{SNR}=30$  dB and for several  $\theta_{\max}$ . It is seen that as  $K$  increases, the array tends to null the desired signal more. The smaller the pointing error  $\theta_{\max}$ , the larger  $K$  must be to null the desired signal to a given level. In the other curves presented in this paper, we have used  $K=0.1$  as a representative value.

Now consider the situation when interference is present. Figure 7 shows a set of curves similar to those in Figure 2 except that interference is incident at  $\theta_i=50^\circ$  with an INR of 40 dB and zero bandwidth ( $B_i=0$ ). These curves differ from those in Figure 2 in several respects. First, for  $\text{SNR}<10$  dB,  $\theta_{\max}$  has less effect on the SINR (except for  $\theta_{\max}$  near  $\theta_i$ ) than it did with no interference. Second, for higher SNRs the SINR again becomes sensitive to  $\theta_{\max}$ , but much less so than without interference. For example, in Figure 7, with  $\text{SNR} = 40$  dB,  $\text{SINR}>0$  dB for  $-38^\circ<\theta_{\max}<22.5^\circ$ , whereas in Figure 2,  $\text{SNR} = 40$  dB yields  $\text{SINR}>0$  dB only for  $-2.9^\circ<\theta_{\max}<2.9^\circ$ . The reason for this difference is that, with interference present, the single degree of freedom in the array pattern is used to form the interference null. The array cannot null the desired signal, as it could without the interference. Finally, with interference present, the output SINR drops precipitously for all SNR's as  $\theta_{\max}$  approaches  $\theta_i$ . Without interference, there is no such critical angle.

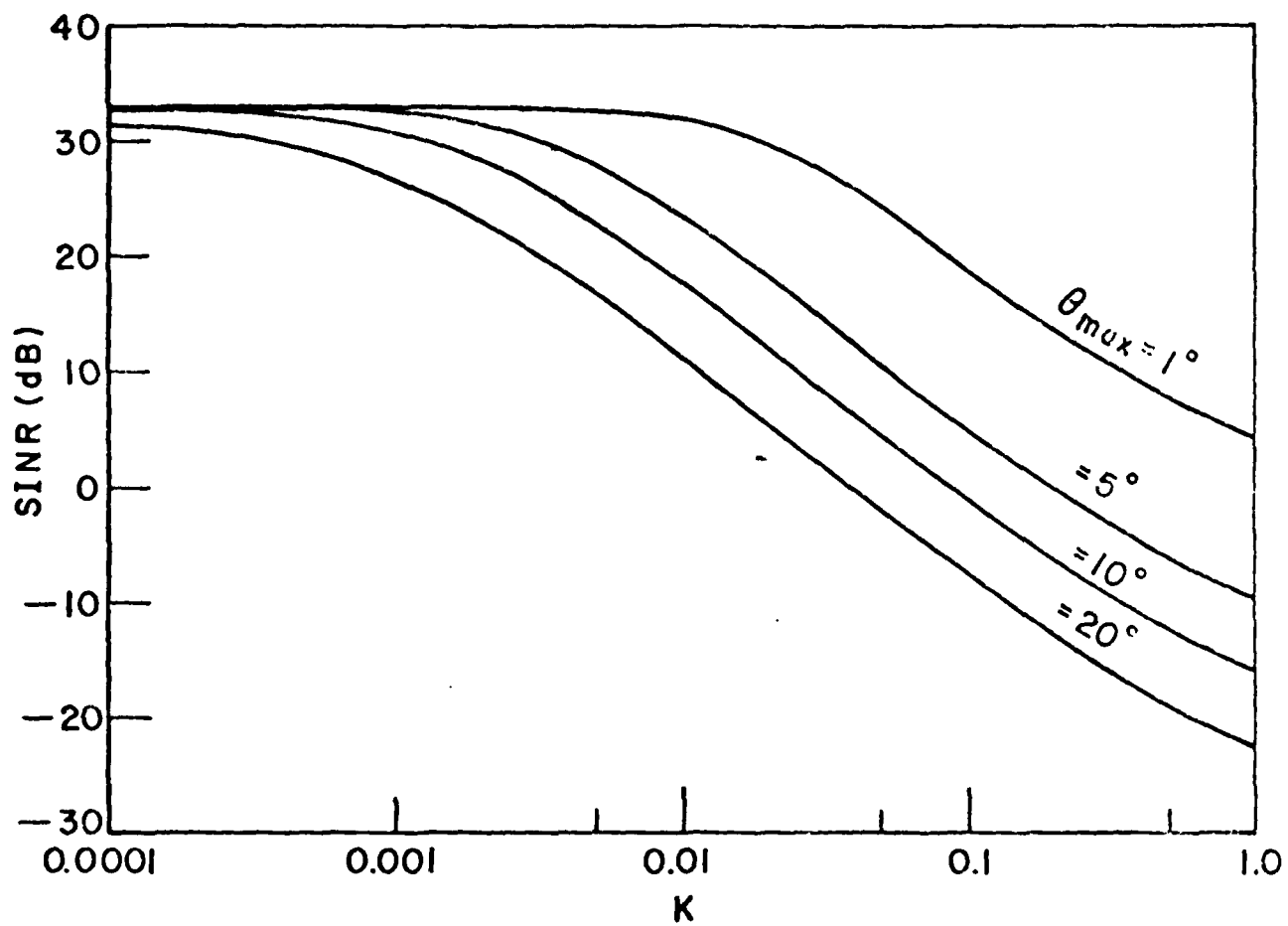


Figure 6. SINR vs. K.  
 $\theta_d=0^\circ$ , SNR=30 dB,  $B_d=0$ .  
 No interference.



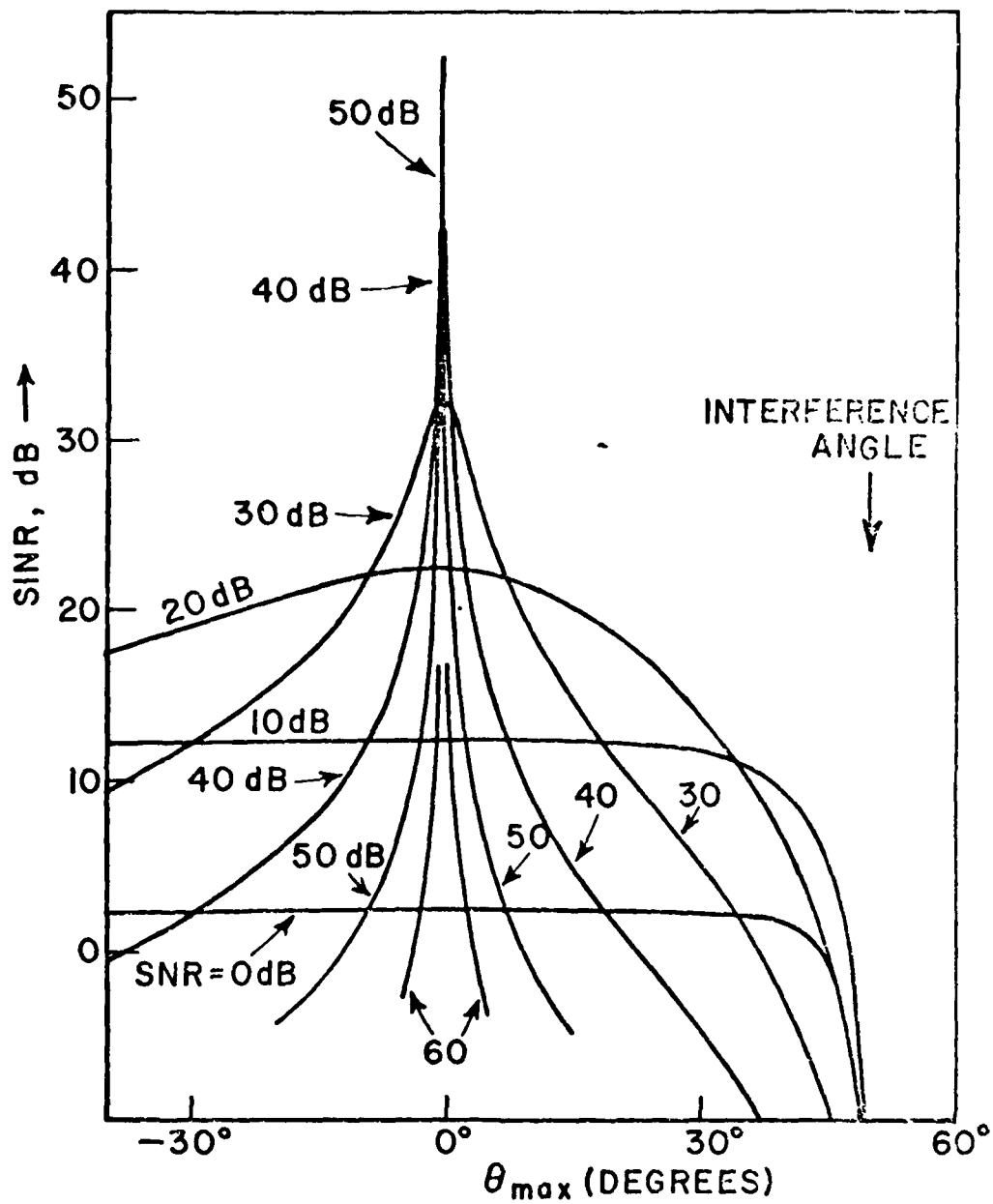


Figure 7. Steered beam array performance.  
 $\theta_d=0^\circ$ ,  $\theta_i=50^\circ$ ,  $B_d=0$ ,  $B_i=0$ ,  $K=.1$ ,  $INR=40$  dB.

Figure 8 shows the corresponding pattern behavior. For  $\text{SNR}=0$  dB and  $\theta_{\max} = 0^\circ$ , the array nulls the interference, as shown. We note that because the array can form only one null, it cannot null both the desired and interference signals. Hence, as the desired signal power is increased, the array responds by reducing the absolute magnitude of the pattern. This behavior may be seen in Figure 8 by comparing the patterns for  $\text{SNR} = 0$  dB and  $\text{SNR} = 20$  dB, for  $\theta_{\max} = 0^\circ$ .

The effect of shifting  $\theta_{\max}$  toward  $\theta_i$  may also be seen in Figure 8 for  $\text{SNR} = 20$  dB. Since  $\text{INR} > \text{SNR}$ , the null remains on the interference. As a result, the more  $\theta_{\max}$  differs from  $\theta_d$ , the more the pattern magnitude is reduced.

Figure 9 shows the output SINR versus the input SNR, for several values of  $\theta_{\max}$ . Also, Figure 9 shows the effect of  $B_i$ , the interference bandwidth. Again, we may compare the performance of the steered beam adaptive array with both the power inversion array and the LMS array. (The LMS array performance is the same as that shown for  $\theta_{\max} = 0^\circ$ .) As was the case without interference, for small SNR,  $\theta_{\max}$  can be far from  $\theta_d$  ( $0^\circ$ ) without degrading performance. As the SNR is increased, however,  $\theta_{\max}$  must be closer and closer to  $\theta_d$  to yield the performance of the LMS array. At high SNR's extremely accurate knowledge of  $\theta_d$  will be needed to achieve top performance. If we compare the steered beam results with those for the power inversion array, we find that the SINR exceeds that of the power inversion array as long as  $\theta_{\max} < 22.5^\circ$ , i.e., as long as  $\theta_{\max}$  is closer to  $\theta_d$  than  $\theta_i$ . Again, our knowledge of  $\theta_d$  does not need to be very accurate to improve on power inversion.

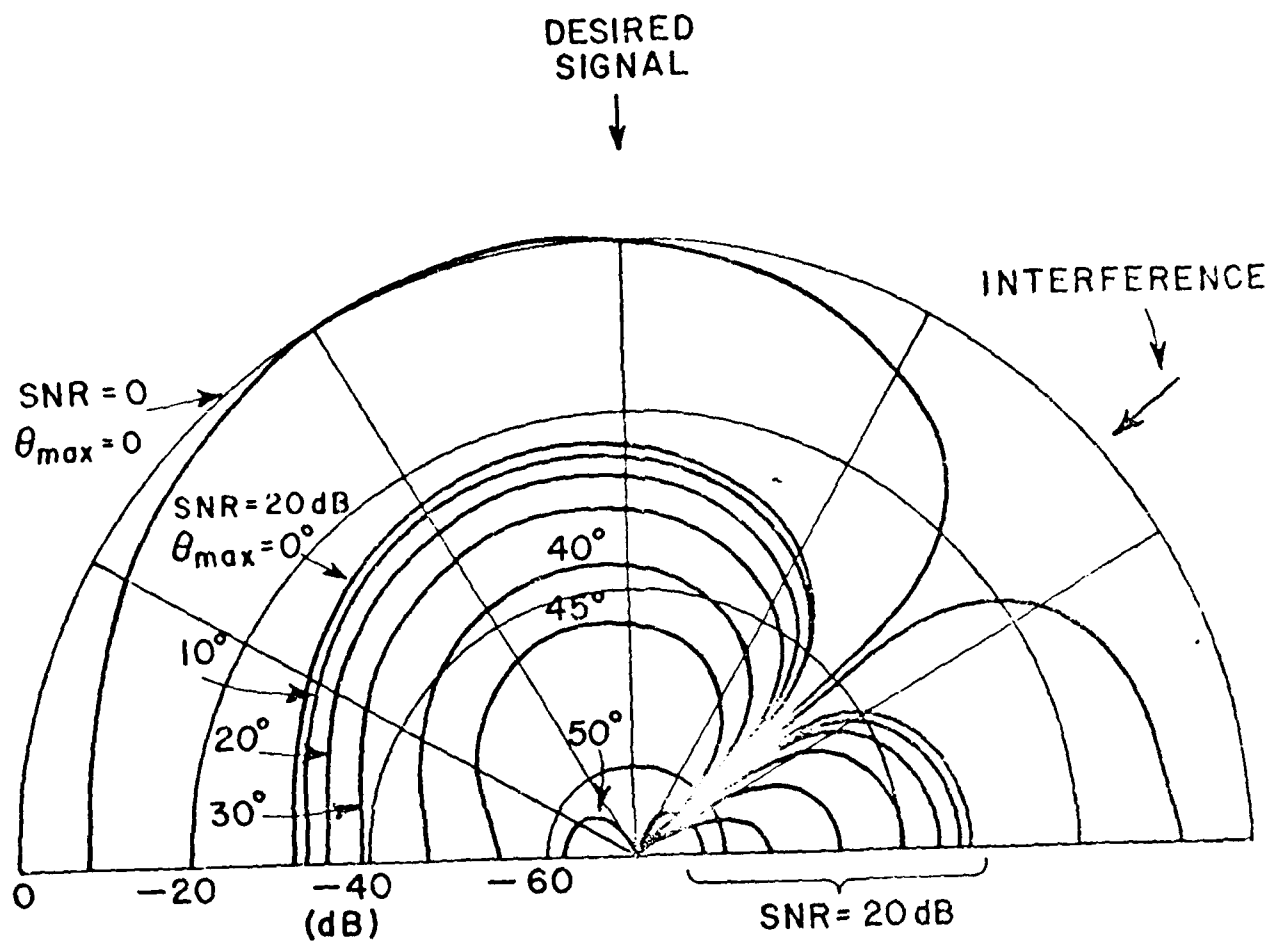


Figure 8. Array pattern.

$B_d = 0$ ,  $\theta_d = 0^\circ$ ,  $K = 0.1$ ,  
 $B_i = 0$ ,  $\theta_i = 50^\circ$ ,  $INR = 40$  dB.



The effect of reducing the angle between  $\theta_d$  and  $\theta_i$  may be seen in Figures 10 and 11. Figure 10 shows SINR versus SNR for  $\theta_i = 30^\circ$  and Figure 11 shows similar results for  $\theta_i = 10^\circ$ . In both cases we find that we must have  $\theta_{\max} < \frac{\theta_i}{2}$  for the system to perform as well as a power inversion array.

The effect of the INR on these results may be seen in Figures 12 and 13. These plots show the output SINR versus input SNR with INR=0 dB and 20 dB, respectively, and  $\theta_i = 50^\circ$ . For INR = 20 dB (Figure 13), we still find (as at higher INR's) that the performance will exceed that of the power inversion array as long as  $\theta_{\max} < \frac{\theta_i}{2}$ . But for INR = 0 dB (Figure 12), the performance is returning to that shown in Figure 5 for no interference.

#### IV. CONCLUSIONS

We have examined the performance of a 2-element steered beam adaptive array as a function of beam pointing error, and have compared this performance with that of an LMS array and a power inversion array. The results show that:

- (1) Without interference, the steered beam array performance exceeds that of the power inversion array as long as the pointing error is less than  $30^\circ$ .
- (2) With interference, the steered beam array performance exceeds that of the power inversion array as long as the beam pointing angle is closer to the desired signal than the interference.

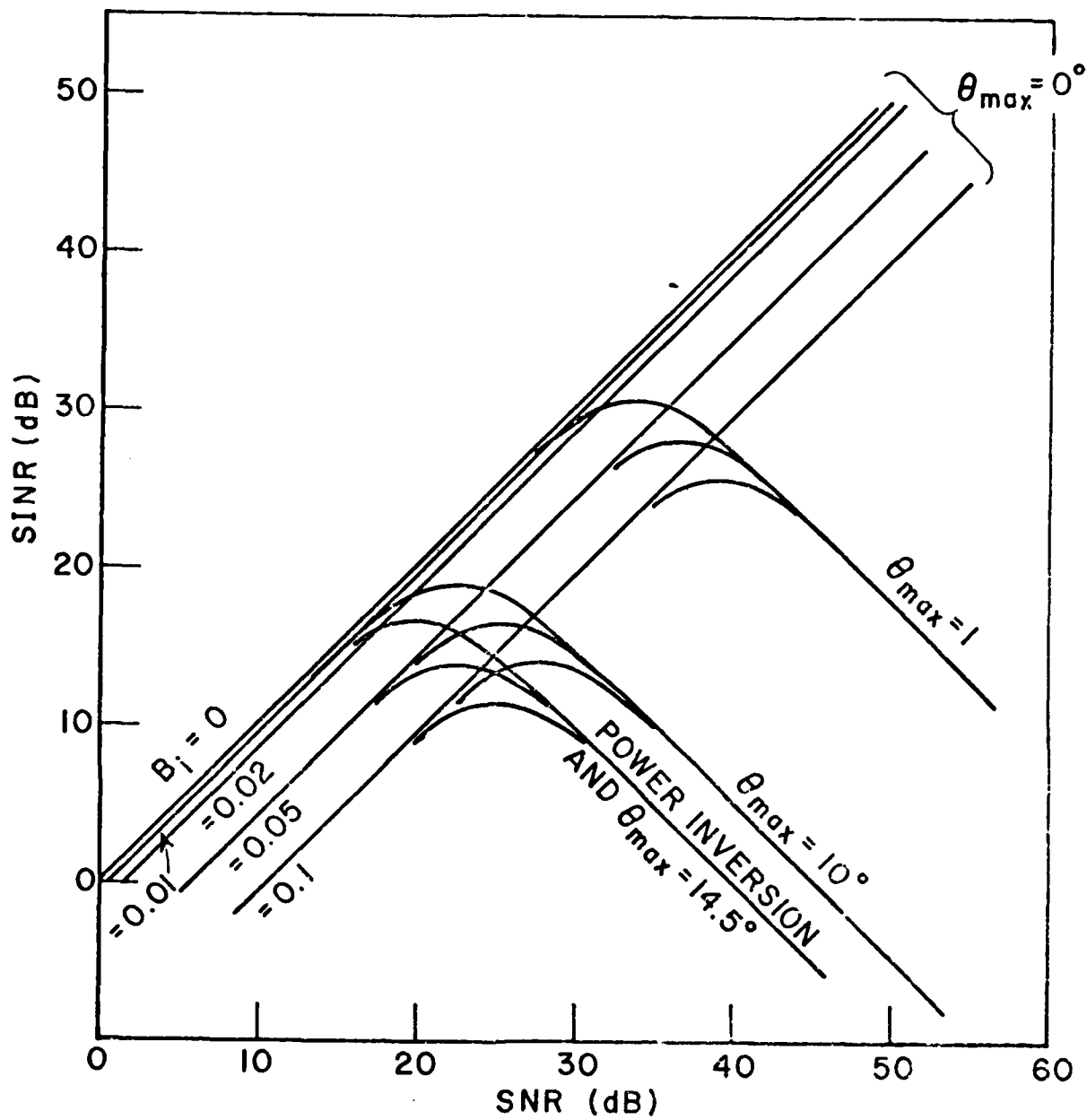


Figure 10. Steered beam array performance.  
 $\theta_d = 0^\circ$ ,  $\theta_i = 30^\circ$ ,  $K = 0.1$ ,  $B_d = 0$ ,  $INR = 40$  dB.

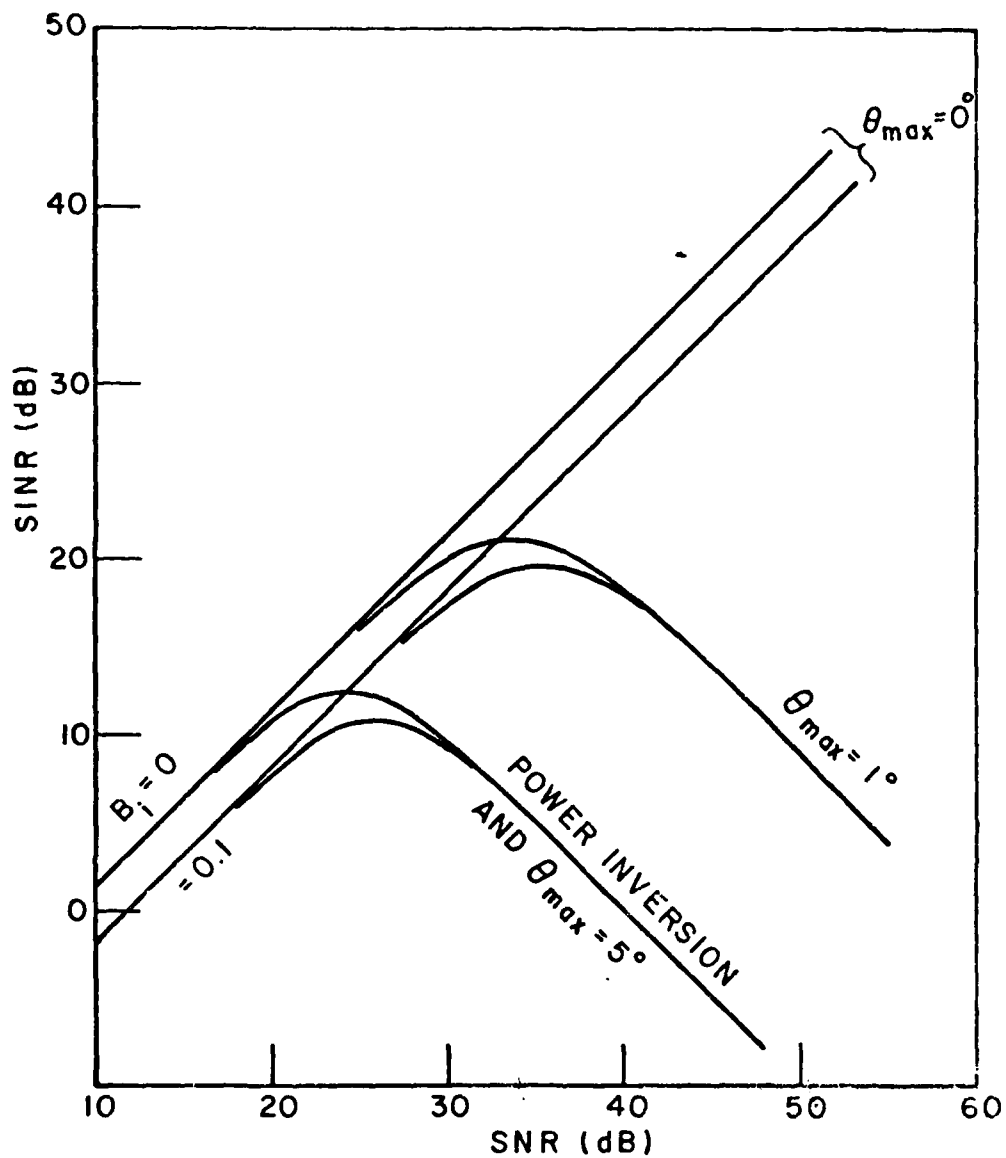


Figure 11. Steered beam array performance.

$\theta_d = 0^\circ$ ,  $\theta_i = 10^\circ$ ,  $K = .1$ ,  $B_d = 0$ ,  $\text{INR} = 40 \text{ dB}$ .

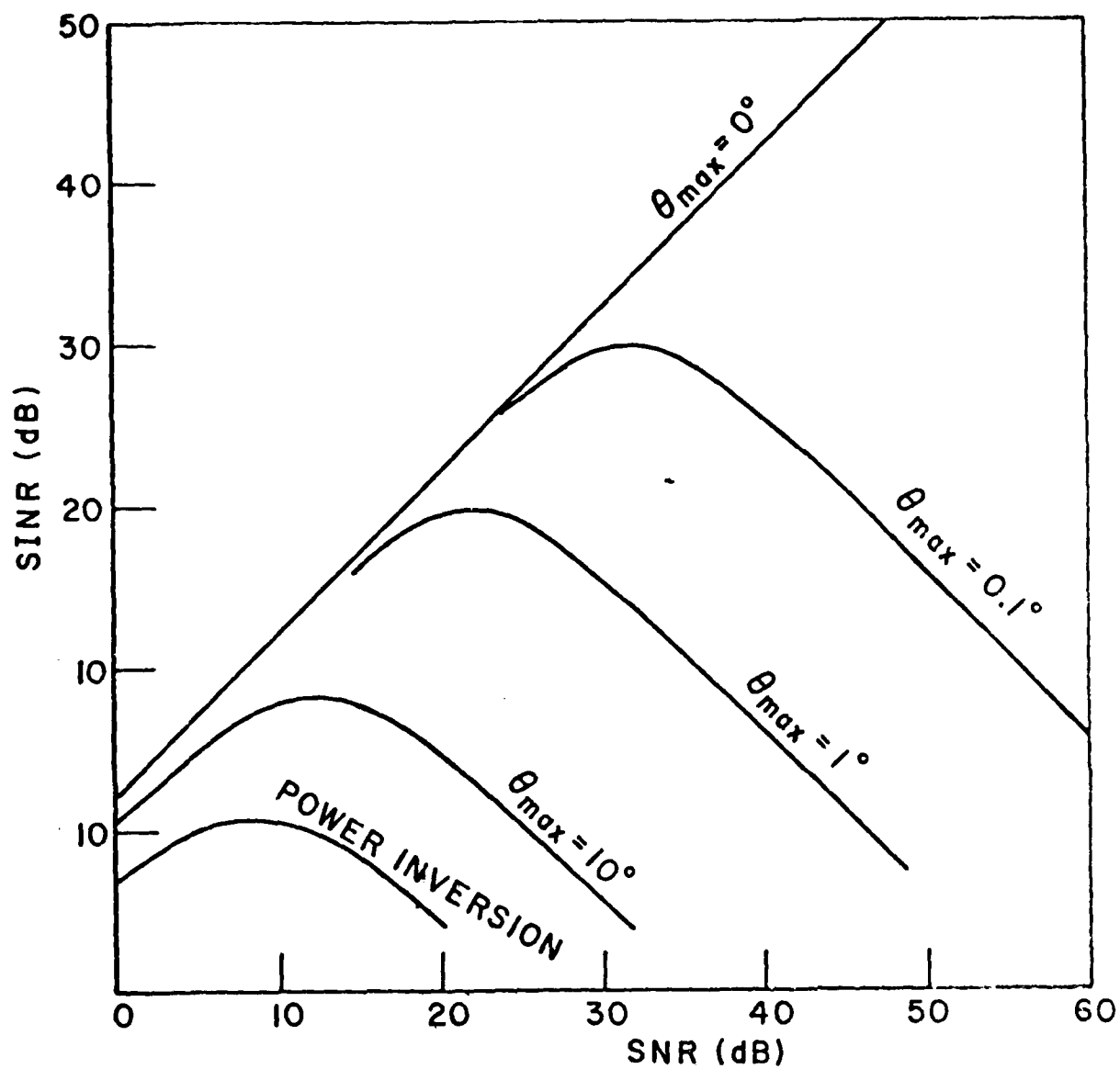


Figure 12. Steered beam array performance.

$\theta_d = 0^\circ$ ,  $\theta_i = 50^\circ$ ,  $K = 0.1$ ,  $INR = 0$  dB,

$B_d = 0$ ,  $0 \leq B_i \leq 2$ .



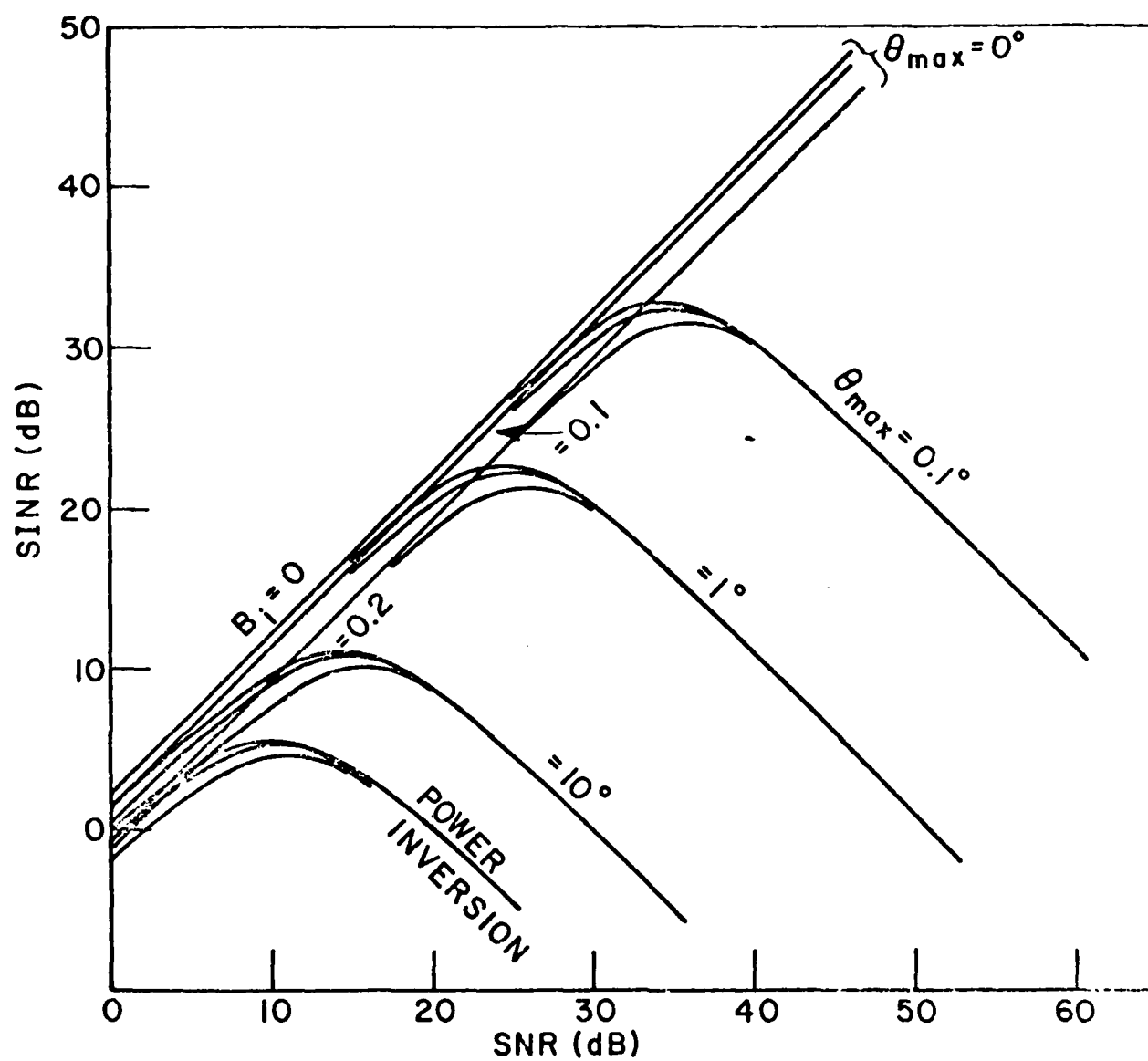


Figure 13. Steered beam array performance.  
 $\theta_d = 0^\circ$ ,  $\theta_i = -50^\circ$ ,  $K = 0.1$ ,  $B_d = 0$ ,  $\text{INR} = 20$  dB.

- (3) For any given beam pointing error, the performance of the steered beam, LMS and power inversion arrays is essentially the same for low SNR (input desired signal-to-noise ratio). But for high SNR, the steered beam array performance is substantially poorer than that of the LMS array unless the beam pointing angle is extremely accurate. The accuracy required depends on the interference power and arrival angle, as shown in Figures 2-13. For example, Figure 9 shows that for  $\text{INR} = 40 \text{ dB}$ ,  $\theta_i = 50^\circ$ ,  $B_i = 0$ , and  $\text{SNR} = 40 \text{ dB}$ , the pointing error must be less than about  $0.1^\circ$  for the steered beam array to do as well as the LMS array.

## REFERENCES

1. B. Widrow, P. E. Mantey, L.J. Griffiths and B.B. Goode, "Adaptive Antenna Systems," Proc. IEEE, 55, December 1967, p. 2143.
2. S.P. Applebaum, "Adaptive Arrays," IEEE Trans., AP-24, September 1976, p. 585.
3. R.L. Riegler and R.T. Compton, Jr., "An Adaptive Array for Interference Rejection," Proc. IEEE, 61, June 1973, p. 748.
4. R.T. Compton, Jr., R.J. Huff, W.G. Swarner and A.A. Ksienski, "Adaptive Arrays for Communication Systems: An Overview of Research at the Ohio State University," IEEE Trans., AP-24, September 1976, p. 599.
5. R.T. Compton, Jr., "An Adaptive Array in a Spread Spectrum Communication System," Proc. IEEE, 66, March 1978, p. 289.
6. R.T. Compton, Jr., "The Power Inversion Adaptive Array - Concept and Performance," IEEE Trans., AES-15, November 1979, p. 803.
7. R.C. Davis, L.E. Brennan and I.S. Reed, "Angle Estimation with Adaptive Arrays in Extended Noise Fields," IEEE Trans., AES-12, March 1976, p. 179.
8. C.L. Zahm, "Effects of Errors in the Direction of Incidence on the Performance of an Adaptive Array," Proc. IEEE (Correspondence), 60, August 1972, p. 1008.